

THE UNIVERSITY OF MICHIGAN RESEARCH INSTITUTE
ANN ARBOR

A GRAPHICAL METHOD FOR MEASURING
DIELECTRIC CONSTANTS AT MICROWAVE FREQUENCIES

Technical Report No. 94

Electronic Defense Group
Department of Electrical Engineering

By: C. B. Sharpe

Approved by:


A. B. Macnee

Project 2899

TASK ORDER NO. EDG-4
CONTRACT NO. DA-36-039 sc-78283
SIGNAL CORPS, DEPARTMENT OF THE ARMY
DEPARTMENT OF ARMY PROJECT NO. 3-99-04-106

September 1959

TABLE OF CONTENTS

	<u>Page</u>
LIST OF ILLUSTRATIONS	iii
ABSTRACT	iv
INTRODUCTION	1
THEORY	4
GRAPHICAL ANALYSIS	8
ILLUSTRATIVE EXAMPLE	13
APPENDIX	18
BIBLIOGRAPHY	20
DISTRIBUTION LIST	21

LIST OF ILLUSTRATIONS

Figure 1	Dielectric Sample in a Waveguide and its Equivalent Circuit	2
Figure 2	Construction of Γ_D , and Γ_I , and Determination of Reference Angle θ_A	9
Figure 3	Shift of Reference Planes and Construction of Γ_F	11
Figure 4	Graphical Determination of the Image Circle and the Iconocenter	14
Figure 5	Construction of Γ_D , and Γ_I	16
Figure 6	Construction of Γ_F	17
Figure 7	Cascade Connection of Linear, Bilateral Two-Port Networks	20

ABSTRACT

This paper describes a graphical method for measuring the real and imaginary parts of the dielectric constant, $\epsilon/\epsilon_0 = \epsilon' - j\epsilon''$, of materials at microwave frequencies. The method is based on the network approach to dielectric measurements proposed by Oliner and Altschuler in which the dielectric sample fills a section of transmission line or waveguide. In contrast to their method, the network representing the dielectric sample is analysed in terms of the bilinear transformation,

$$\Gamma' = \frac{a\Gamma + b}{c\Gamma + d}; \quad ad - bc = 4$$

The analysis proceeds from the geometric properties of the image circle in the Γ -plane obtained by terminating the output line in a calibrated sliding short.

The technique described retains the desirable features of the network approach but avoids the necessity of measuring both scattering coefficients. As a result the procedure is more direct and, in the case of the TEM configuration, leads to an entirely graphical solution in which the complex dielectric constant can be read from a Smith chart overlay.

A GRAPHICAL METHOD FOR MEASURING
DIELECTRIC CONSTANTS AT MICROWAVE FREQUENCIES

INTRODUCTION

There are many techniques for making dielectric measurements at microwave frequencies.¹ One of the more interesting methods proposed in recent years is that due to Oliner and Altschuler², in which the dielectric sample filling a section of wave guide is represented by a two-port microwave network as illustrated in Fig. 1. In their method the scattering matrix of the network is determined at reference planes T_1 and T_2 by Deschamps'³ procedure or, when the network can be regarded as lossless, by alternative so-called precision techniques. The complex relative dielectric constant $\epsilon/\epsilon_0 = \epsilon' - j\epsilon''$ is then obtained from either

$$\epsilon/\epsilon_0 = (Y/Y_0)^2 \text{ (TEM modes)} \quad (1a)$$

or

$$\epsilon/\epsilon_0 = \frac{(Y/Y_0)^2 + (\lambda_{og}/\lambda_c)^2}{1 + (\lambda_{og}/\lambda_c)^2} \text{ (H modes)}, \quad (1b)$$

where the wave admittance Y in the dielectric relative to the wave admittance of the empty guide, Y_0 , is given in terms of the scattering coefficients by

$$(Y/Y_0)^2 = \frac{(1 - S_{11})^2 - S_{12}^2}{(1 + S_{11})^2 - S_{12}^2}, \quad (2)$$

and λ_{og} and λ_c refer to the guide wavelength and the cutoff wavelength, respectively, in the air-filled guide.

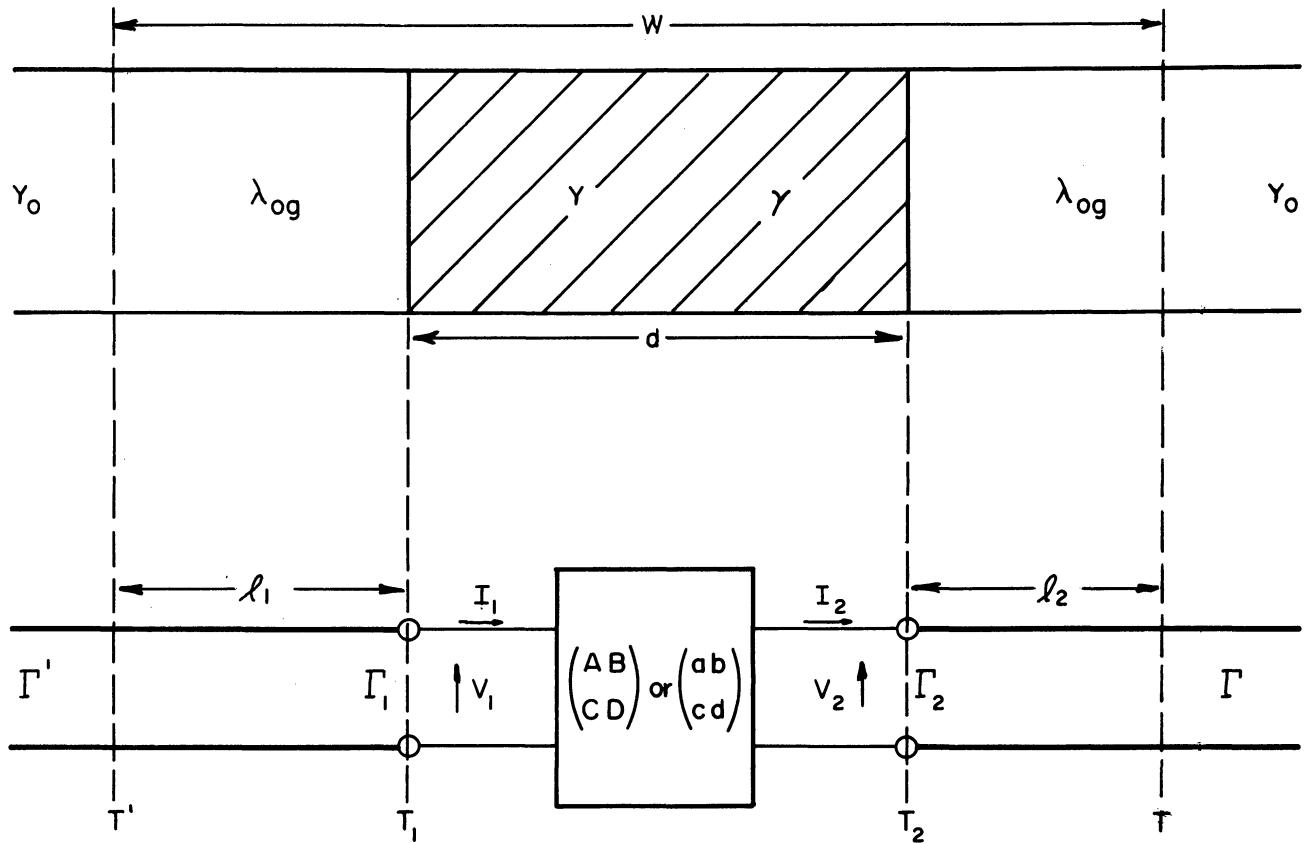


FIG.1 DIELECTRIC SAMPLE IN A WAVEGUIDE AND ITS EQUIVALENT CIRCUIT

Oliner and Altschuler point out that the introduction of the network point of view to dielectric measurements results in two major advantages over earlier methods. First, it becomes possible to employ precision techniques in the determination of the network parameters. For example, in Deschamps' geometrical method the image circle, representing the locus of points in the input reflection coefficient plane as a sliding short is moved in the output waveguide, is determined by graphical averaging. Therefore, the center of the image circle and its radius, as well as quantities derived from them, can be determined to a higher degree of precision than that of a single data point. The second feature of the network method which can be exploited to advantage in dielectric measurements concerns the concept of invariance. Briefly stated, invariance in the present case refers to the method of microwave network representation or measurement which calls for a minimum number of physical length measurements. Thus, for the configuration illustrated in Fig. 1 it is possible to take advantage of the known symmetry of the network to reduce to one the number of required distance measurements. The single measurement required may be either the length of the sample, d , (location invariant) or the location of the one of the sample faces, T_1 or T_2 (length invariant). The desirability of employing a distance invariant method lies in the fact that errors arising from physical distance measurements are generally greater than those resulting from the electrical distance measurements, assuming that corrections have been made for errors in the location of the voltage minimum due to spurious discontinuities if they exist.

The purpose of the present paper is to describe a technique for measuring dielectric constants which retains the desirable features of the network approach but which can be accomplished more directly and with a minimum of computation. In the case of the TEM configuration, the dielectric constant can be obtained by a purely graphical procedure in which the desired complex constant is read directly from a Smith Chart.

THEORY

The dielectric-filled section of line or waveguide can be represented at reference planes T_1 and T_2 by the (ABCD) circuit parameters which relate the input and output voltages and currents, as defined in Fig. 1, by the matrix equation:

$$\begin{bmatrix} V_1 \\ I_1 \end{bmatrix} = \begin{bmatrix} A & B \\ C & D \end{bmatrix} \begin{bmatrix} V_2 \\ I_2 \end{bmatrix}, \quad (3)$$

where $AD-BC = 1$. If we take

$$Z_1 = V_1/I_1, \quad Z_2 = V_2/I_2, \quad (4)$$

then a bilinear relationship is obtained between the impedances Z_1 and Z_2 :

$$Z_1 = \frac{AZ_2 + B}{CZ_2 + D}. \quad (5)$$

This transformation has often been used in analyzing the properties of linear two-port networks. However, it will be more convenient in the present case to consider the network representing the dielectric sample in terms of a bilinear transformation in the reflection coefficient or Γ -plane. Thus, if the input and output reflection coefficients are defined, respectively, by

$$\Gamma_1 = \frac{Y_0 - Y_1}{Y_0 + Y_1}; \quad \Gamma_2 = \frac{Y_0 - Y_2}{Y_0 + Y_2}, \quad (6)$$

it can be shown that

$$\Gamma_1 = \frac{a\Gamma_2 + b}{c\Gamma_2 + d}, \quad (7)$$

where

$$\begin{aligned} a &= A - BY_0 - C/Y_0 + D \\ b &= A + BY_0 - C/Y_0 - D \\ c &= A - BY_0 + C/Y_0 - D \\ d &= A + BY_0 + C/Y_0 + D \end{aligned} \quad (8)$$

Reciprocity is assured if $ad - bc = 4$. If the network is symmetrical, as in the present case, then $b = -c$. Equation 7 is sometimes called the direct transformation to distinguish it from the inverse transformation,

$$\Gamma_2 = \frac{-d\Gamma_1 + b}{c\Gamma_1 - a} \quad (9)$$

The matrix composed of the (abcd) parameters might be termed the reflection matrix of the network. Although the transformation (7) has been used by Mathis⁴ and also by Bolinder⁵ employing a different normalization, it has not enjoyed widespread use as a tool in network analysis. As would be expected, the reflection matrix bears a close connection to the scattering matrix. It can be shown that in general

$$S = \begin{bmatrix} S_{11} & S_{12} \\ S_{21} & S_{22} \end{bmatrix} = \begin{bmatrix} b/d & 2/d \\ (ad-bc)/2d & -c/d \end{bmatrix}. \quad (10)$$

An obvious application of (10) is suggested in the appendix. The components of the reflection matrix transform in a manner very similar to the manner in which the scattering coefficients transform as a result

of a shift in reference planes. Referring to Fig. 1 the reflection matrix at reference planes T' and T is given by

$$\begin{bmatrix} a' & b' \\ c' & d' \end{bmatrix} = \begin{bmatrix} e^{-j\phi_1} & 0 \\ 0 & e^{j\phi_1} \end{bmatrix} \begin{bmatrix} a & b \\ c & d \end{bmatrix} \begin{bmatrix} e^{-j\phi_2} & 0 \\ 0 & e^{j\phi_2} \end{bmatrix}, \quad (11)$$

where $\phi_1 = 2\pi l_1/\lambda_{og}$, $\phi_2 = 2\pi l_2/\lambda_{og}$, and the primed coefficients are defined by

$$\Gamma' = \frac{a'\Gamma + b'}{c'\Gamma + d'}. \quad (12)$$

Returning to the problem at hand the (ABCD) matrix of the dielectric-filled section at reference planes T₁ and T₂ is

$$\begin{bmatrix} A & B \\ C & D \end{bmatrix} = \begin{bmatrix} \cosh \gamma d & \frac{\sinh \gamma d}{Y} \\ Y \sinh \gamma d & \cosh \gamma d \end{bmatrix} \quad (13)$$

from which Eqs. (8) yield,

$$\begin{aligned} a &= 2 \cosh \gamma d - (Y/Y_0 + Y_0/Y) \sinh \gamma d \\ b &= -c = -(Y/Y_0 - Y_0/Y) \sinh \gamma d \\ d &= 2 \cosh \gamma d + (Y/Y_0 + Y_0/Y) \sinh \gamma d, \end{aligned} \quad (14)$$

where $\gamma = \alpha + j\beta$ is the propagation constant in the dielectric.

A purely algebraic relation between Y/Y_0 and the (abcd) parameters can be obtained by forming

$$\Gamma_E \equiv \frac{a-d}{2c} = \frac{1 + (Y/Y_0)^2}{1 - (Y/Y_0)^2}. \quad (15)$$

This expression is entirely equivalent to (2) involving the scattering coefficients. The merit of the reflection parameter representation lies in the simplicity of (15) as well as in the facility it provides in the geometric interpretation of the problem. Thus, it will be shown that Γ_E

can be determined through a series of simple geometric constructions based on the image circle diagram. The desired dielectric constant then follows from (1a) or (1b).

In the interest of generality we will proceed from the initial assumption that reference planes T and T' are located arbitrarily with respect to the sample. Equation (12) is first re-written in the form⁶

$$\Gamma' = \frac{a\bar{c}|\Gamma|^2 - b\bar{d}}{c\bar{c}|\Gamma|^2 - d\bar{d}} - \left[\frac{\bar{c}\bar{\Gamma} + \bar{d}}{c\bar{\Gamma} + d} \right] \left[\frac{ad - bc}{c\bar{c}|\Gamma|^2 - d\bar{d}} \right] \Gamma, \quad (16)$$

where the bar over a quantity designates the complex conjugate and the primes have been omitted. One can determine the center of the image circle and its radius from (16) by inspection. Thus, when $|\Gamma| = 1$, corresponding to a reactive termination in the output waveguide, the first term in (16) will be a complex constant and the magnitude of the second term will be a constant for all values of reactance. Referring to Fig. 2 the center of the image circle in the Γ' -plane is

$$\Gamma_{C'} = \frac{a\bar{c} - b\bar{d}}{c\bar{c} - d\bar{d}} \quad (17)$$

and the radius is

$$R = \frac{4}{|c\bar{c} - d\bar{d}|}. \quad (18)$$

There are three points in the reflection plane which are of special interest. The iconocenter, $\Gamma'_{0'} = S_{11} = b/d$, is the map or image of $\Gamma = 0$ in the Γ' -plane. There are a number of geometric constructions which can be used to obtain the iconocenter once the image circle and its center are known.^{7,8,9,10} All of these methods make use of a calibrated short behind the network, and all but the last method referenced depend on a knowledge of the wavelength in the

output waveguide. The other two points of interest in the reflection plane are $\Gamma_{D'} = a/c$ and $\Gamma_{I'} = -d/c$. These points have a special significance in the theory of the bilinear transformation and can be shown to mark the center of the isometric circles for the direct and inverse transformations, respectively.¹¹

GRAPHICAL ANALYSIS

Once $\Gamma_{O'}$ and $\Gamma_{C'}$ are determined $\Gamma_{D'}$ can be readily constructed by inverting $\Gamma_{O'}$ with respect to the image circle as illustrated in Fig. 2. The proof of this statement is contained in

$$(\Gamma_{D'} - \Gamma_{C'}) (\bar{\Gamma}_{O'} - \bar{\Gamma}_{C'}) = R^2, \quad (19)$$

which follows from (17), (18), and the condition, $ad-bc = 4$. The construction of the point $\Gamma_{I'}$ follows in an analogous way, although in contrast to the previous case, the angle of $\Gamma_{I'}$ will depend on the choice of the output reference plane T. It is convenient at this point to locate T symmetrically with respect to T' so that $l_1 = l_2$. Assuming for the moment that T has been so located, the symmetry of the network representing the dielectric then guarantees that $b = -c$, and $\Gamma_{I'}$ can be determined graphically by constructing the reciprocal of $\Gamma_{O'}$. This construction is also illustrated in Fig. 2. It is interesting to note that $\Gamma_{I'}$ is also the inverse with respect to the unit circle of $\Gamma_C = -\bar{c}/\bar{d}$, which is the map in the output Γ -plane of the center of the image circle, $\Gamma_{C'}$, via the inverse transformation (9).

The location of T is accomplished by noting that when $b = -c$ the point $A = -1$ maps into A' at

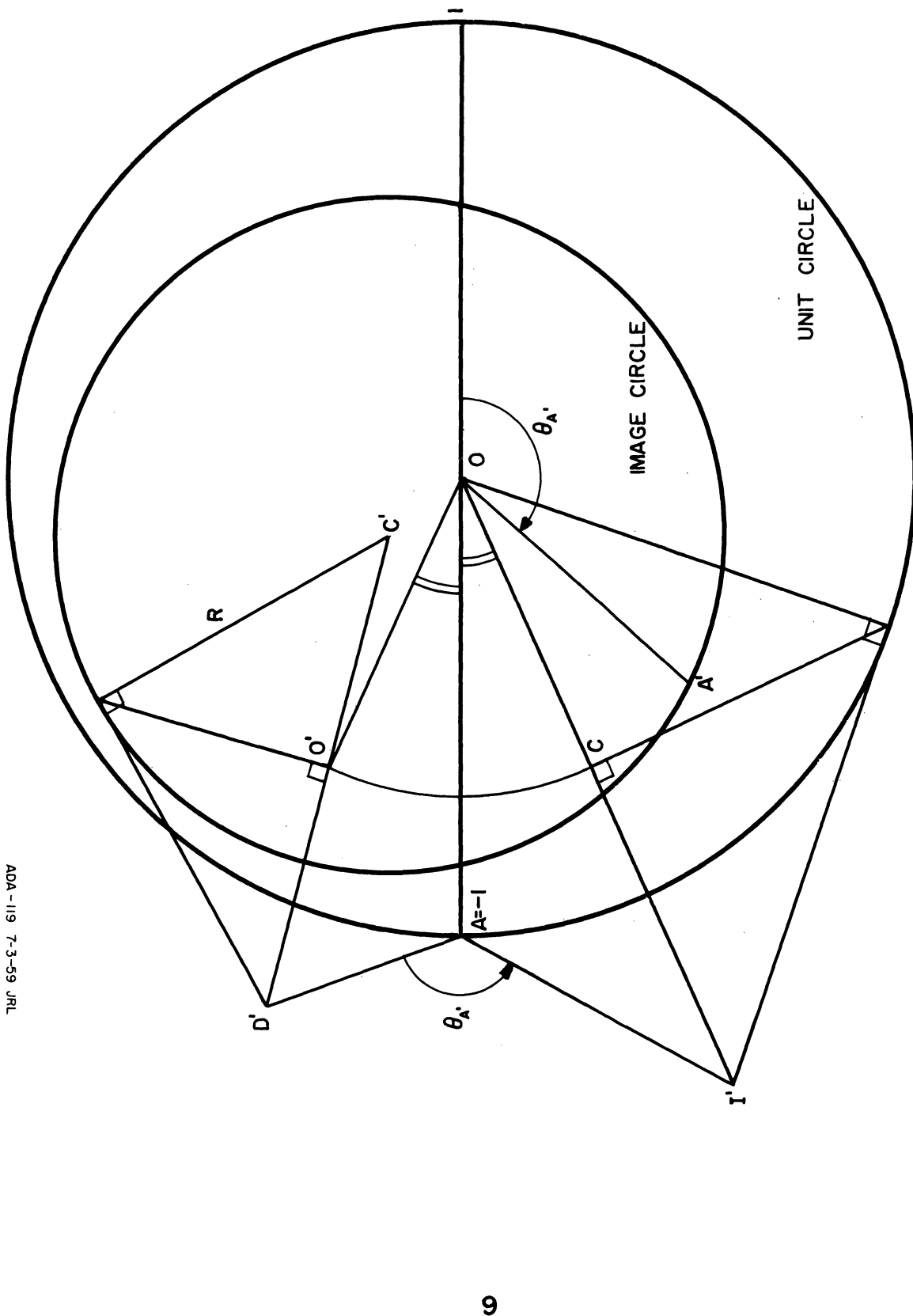


FIG. 2 CONSTRUCTION OF I' & I'' AND DETERMINATION OF REFERENCE ANGLE $\theta_{A'}$

$$\Gamma_{A'} = \frac{1 + \Gamma_{D'}}{1 + \Gamma_{I'}} \quad (20)$$

The reference point A' on the image circle is determined by the angle $\theta_{A'} = \arg \Gamma_{A'}$, which can be constructed from $\Gamma_{D'}$ and $\Gamma_{I'}$, as shown in Fig. 2. Thus, in order to guarantee symmetry one locates T at that position of the short in the output waveguide which establishes a voltage minimum at a distance $l = (\pi - \theta_{A'}) \lambda_{og} / 4\pi$ from T' toward the generator in the input waveguide. It should be noted that this procedure establishes T only to within a multiple of half a wavelength. However, an approximate knowledge of the location of the sample suffices to remove any ambiguity.

At this point it is desirable to distinguish between the location invariant and the length invariant procedures. In the location invariant procedure T' is located at an arbitrary point in the input waveguide, and T is determined from symmetry considerations as described above. The distance to the sample faces is calculated from $l_1 = l_2 = (w-d)/2$, where w and d are defined in Fig. 1 and are assumed to be known. It then remains to transform $\Gamma_{D'}$ and $\Gamma_{I'}$ to reference planes T_1 and T_2 at the sample faces. If $\Gamma_{D'}$ and $\Gamma_{I'}$ denote the isometric centers relative to planes T' and T, and Γ_D and Γ_I the corresponding quantities relative to planes T_1 and T_2 , then it follows from (11) that

$$\Gamma_D = e^{2j\phi} \Gamma_{D'}; \quad \Gamma_I = e^{-2j\phi} \Gamma_{I'}, \quad (21)$$

where $\phi = (w - d) \pi / \lambda_g$. The transformation of reference planes and the construction of Γ_E , which is the average of Γ and Γ_I , is apparent from Fig. 3. In the case of a TEM structure the desired dielectric constant can be read directly from a Smith Chart overlay, in view of (1a) and (15), by constructing the point

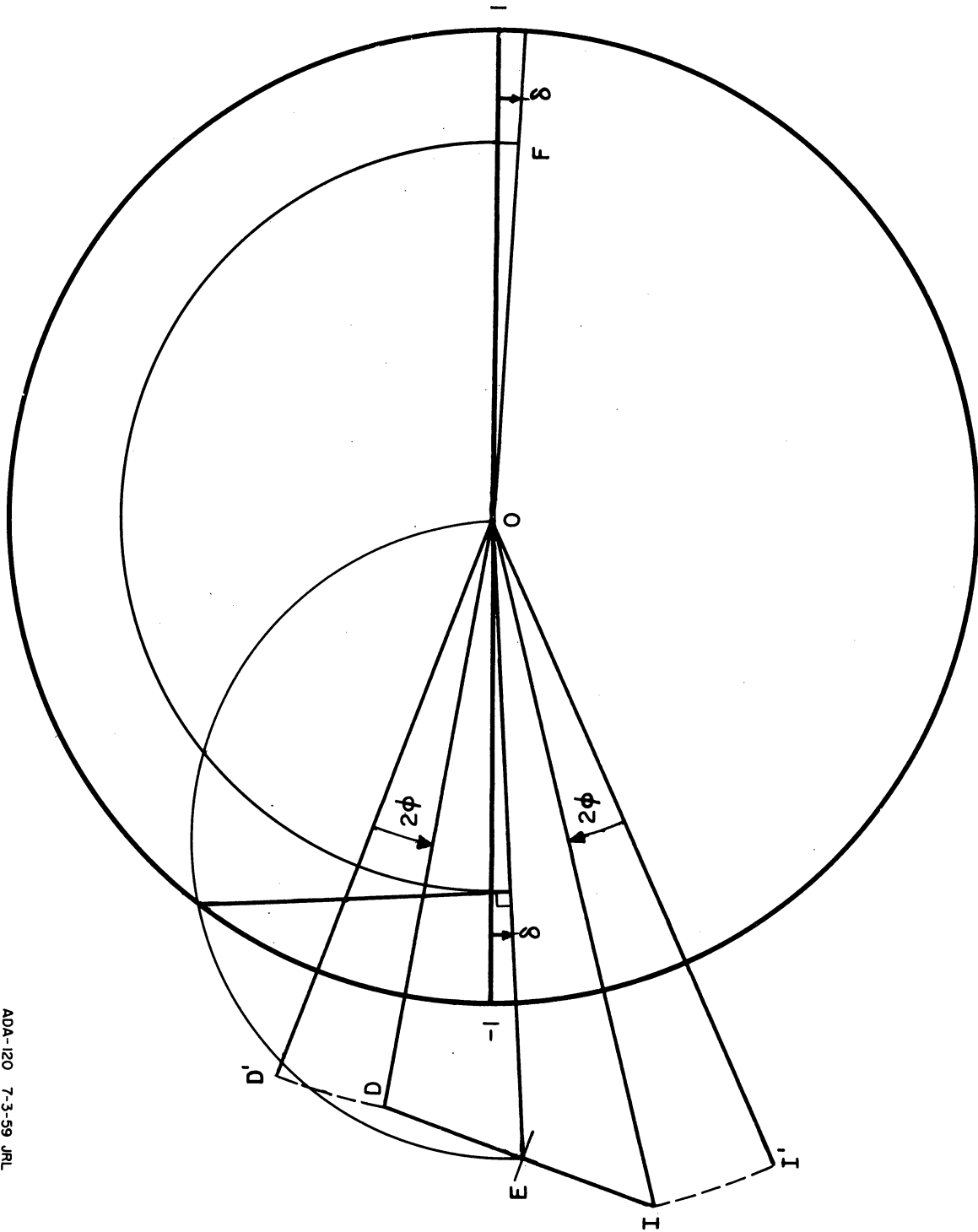


FIG.3 SHIFT OF REFERENCE PLANES AND CONSTRUCTION OF I_F

$$\Gamma_F \equiv -1/\Gamma_E = \frac{\epsilon/\epsilon_0 - 1}{\epsilon/\epsilon_0 + 1}. \quad (22)$$

This construction is also shown in Fig. 3.

In the length invariant procedure one makes the initial assumption that the front face of the sample can be located accurately by physical means, thus making $T' = T_1$. This amounts to a trivial distance determination, which in rectangular waveguides can be readily accomplished by mounting the sample in a shorting switch. Since the analysis proceeds from the assumption of symmetry no distance measurement is required in the length invariant case and the actual location of reference plane T is of no interest. The points Γ_E and Γ_F are derived directly from Γ_D , and Γ_I , as determined in Fig. 2 without shifting reference planes.

When the loss tangent of the dielectric is relatively small the graphical method will give rather poor percentage accuracy in the determination of ϵ'' . In this case it is advisable to determine ϵ'' independently. This can be done most simply by using the already determined image circle to calculate the intrinsic insertion loss of the dielectric.¹² The necessary formulas are listed below for the convenience of the reader. If $\rho = |\Gamma_C|$ is the distance of the center of the image circle from the origin of the reflection plane, it can be shown that

$$2\alpha d = \ln \left[\frac{\sqrt{(1+R)^2 - \rho^2} + \sqrt{(1-R)^2 - \rho^2}}{\sqrt{(1+R)^2 - \rho^2} - \sqrt{(1-R)^2 - \rho^2}} \right]. \quad (23)$$

Knowing ϵ' , the desired ϵ'' is then obtained from either

$$\epsilon'' = 2\left(\frac{\alpha\lambda}{2\pi}\right)^2 \sqrt{1 + \left(\frac{2\pi}{\alpha\lambda}\right)^2} \epsilon' \quad (\text{TEM modes}), \quad (24)$$

where λ is the free space wave length or

$$\epsilon'' \cong \frac{\alpha\lambda_{og}}{\pi} \frac{\sqrt{[1 + (\lambda_{og}/\lambda_c)^2] \epsilon' - (\lambda_{og}/\lambda_c)^2}}{1 + (\lambda_{og}/\lambda_c)^2} \quad (\text{H modes}), \quad (25)$$

if

$$\epsilon'' \ll \epsilon' - \frac{1}{1 + (\lambda_c/\lambda_{og})^2} . \quad (26)$$

ILLUSTRATIVE EXAMPLE

To illustrate the application of the graphical method an example is considered in this section. Measurements were made at 9.330 kmc on a sample of Catalin plastic, .175" thick, which filled the cross-section of an x-band waveguide. The sample was mounted in a shorting switch making it possible to replace quite accurately the front face of the sample with a short. Since T_1 could thus be readily determined the length invariant procedure was employed. The values of reflection coefficient as measured on the input slotted line relative to T_1 as the short was moved through successive positions separated by $\lambda_{og}/16$ are plotted in the polar diagram of Fig. 4. The numbers indicate the sequence of measurements and are not otherwise significant. Shown in the same figure is the construction for the iconocenter, O' . This construction, which is apparent from the figure, is derived and illustrated in Reference 8. It is to be noted that the construction of the auxiliary

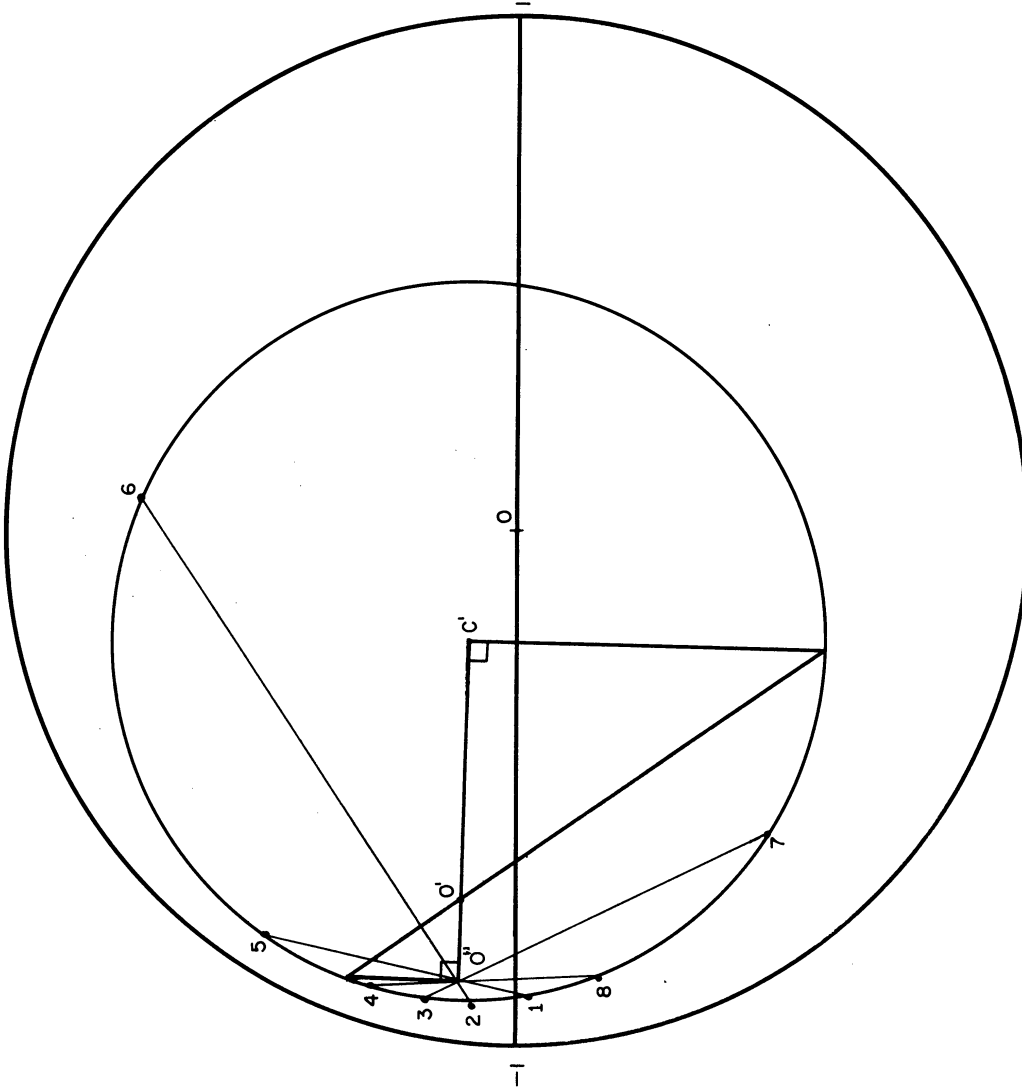


FIG. 4. GRAPHICAL DETERMINATION OF THE
IMAGE CIRCLE AND THE ICONOCENTER.

point O'' is accomplished by drawing straight lines between those points in the input Γ' plane which correspond to opposite ends of a diameter of the unit circle when mapped into the output Γ'' -plane.

Once O' is located the method proceeds as described in the preceding sections. In Fig. 5 the point O' is inverted with respect to the image circle to obtain D' , and C , the conjugate of O' , is inverted with respect to the unit circle to obtain I' . Since symmetry is implied in the construction of I' , the symmetry of the sample insures that D' and I' denote a/c and $-d/c$, respectively, at the sample faces. Figure 6 illustrates the determination of Γ_F . In this example we cannot obtain ϵ/ϵ_0 directly from the Smith chart because we do not have a TEM structure. However, we can still use the Smith chart to obtain $(Y/Y_0)^2$, and then determine ϵ/ϵ_0 from (1b). Reading from the impedance scale at F , $(Y/Y_0)^2 = 8.0 - j1.2$. The value of the guide wavelength was found by measurement to be $\lambda_{og} = 4.542$ cm, and for x-band rectangular waveguide, $\lambda_c = 4.572$ cm. Equation (1b) then yields,

$$\begin{aligned} \epsilon/\epsilon_0 &= \frac{8.0 - j1.2 + \left(\frac{4.542}{4.572}\right)^2}{1 + \left(\frac{4.542}{4.572}\right)^2} \\ &= 4.52 - j0.60 \end{aligned}$$

which agrees well with the published values for Catalin.

It should be pointed out that an expanded reflection plane and Smith chart are necessary if one wishes to retain throughout the graphical procedure the precision inherent in the original electrical measurements.

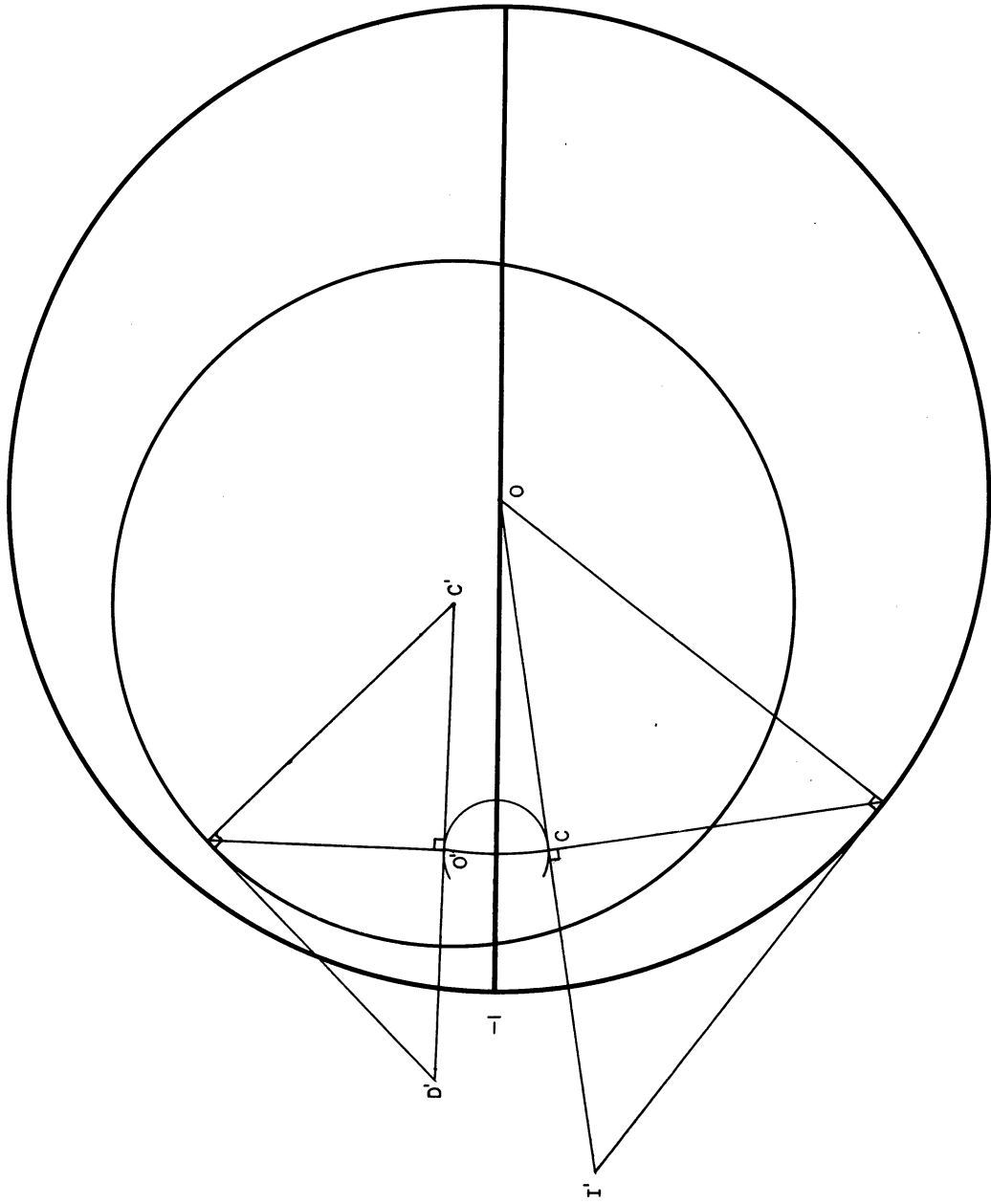


FIG. 5. CONSTRUCTION OF Γ_D AND Γ_I

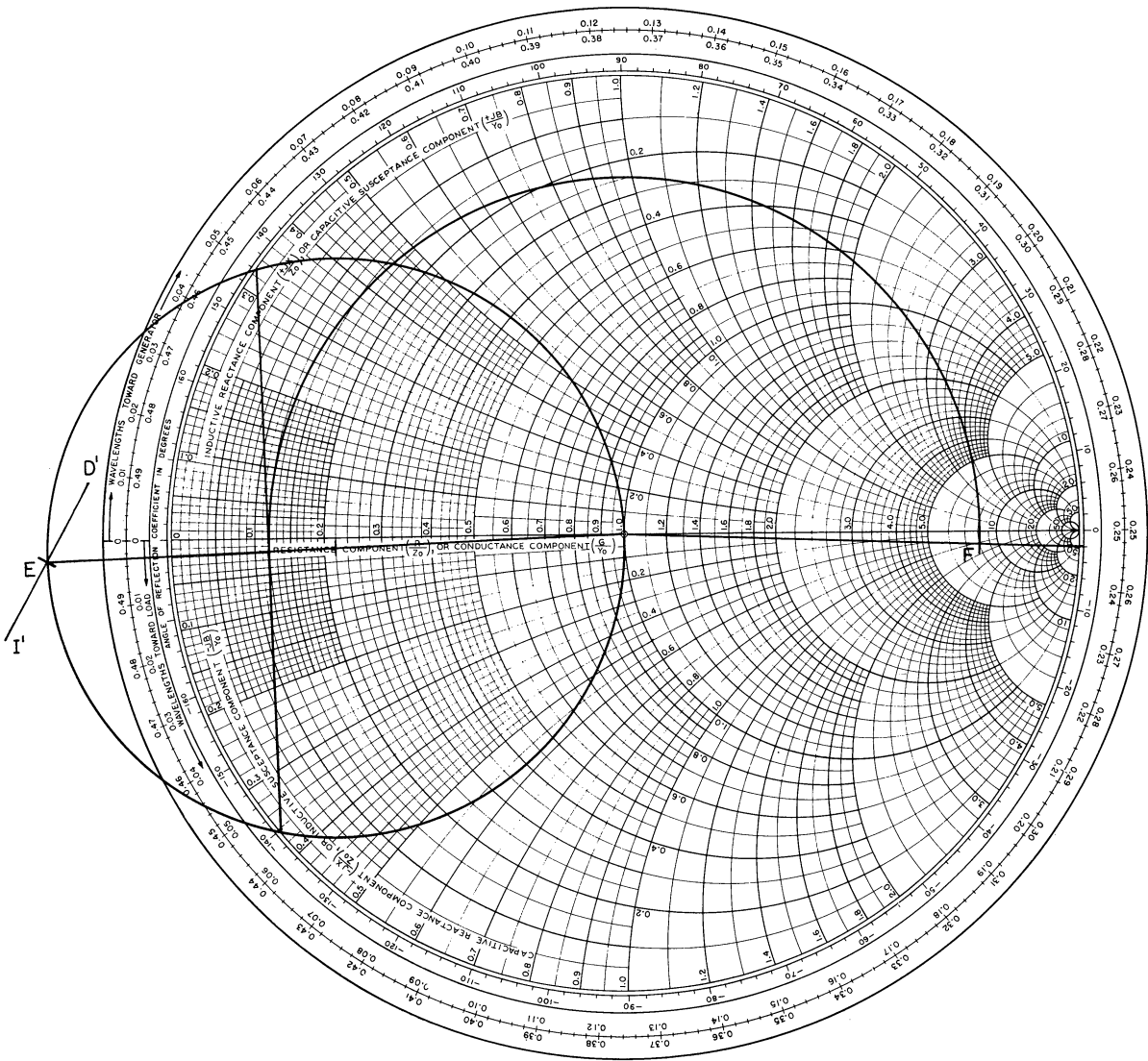


FIG. 6. CONSTRUCTION OF Γ_F

APPENDIX

It is well known that repeated bilinear transformations can be expressed in terms of a matrix product. Thus, if n linear networks are connected in cascade as shown in Fig. 7, the reflection matrix of the combination is given by

$$\begin{bmatrix} 2^{n-1} a & 2^{n-1} b \\ 2^{n-1} c & 2^{n-1} d \end{bmatrix} = \begin{bmatrix} a_1 & b_1 \\ c_1 & d_1 \end{bmatrix} \begin{bmatrix} a_2 & b_2 \\ c_2 & d_2 \end{bmatrix} \dots \begin{bmatrix} a_n & b_n \\ c_n & d_n \end{bmatrix}. \quad (\text{A-1})$$

The factor of 2^{n-1} guarantees that $ad-bc = 4$ if $a_i d_i - b_i c_i = 4$, $i = 1, 2, 3, \dots, n$. The problem of determining the scattering matrix of a cascade connection of networks is, therefore, reduced to a systematic and relatively direct procedure through the use of (A-1) and (10). In this application the reflection matrix bears a close resemblance to the transmission or T-matrix^{1,3} as might have been anticipated from

$$T = \begin{bmatrix} a/2 & -c/2 \\ -b/2 & d/2 \end{bmatrix}, \quad (\text{A-2})$$

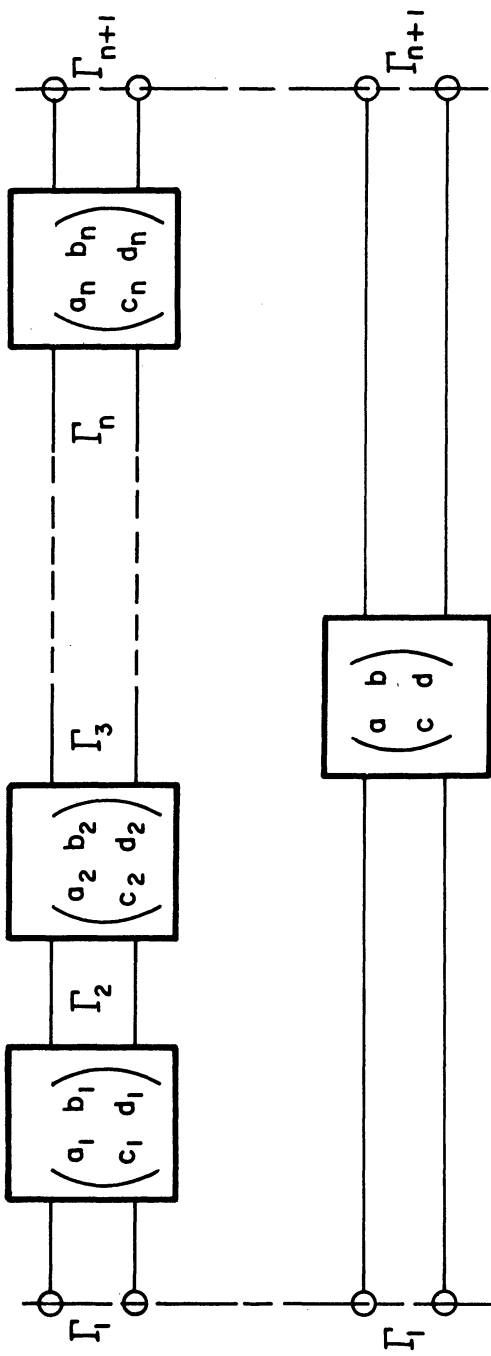


FIG. 7. CASCADE CONNECTION OF LINEAR, BILATERAL TWO-PORT NETWORKS

BIBLIOGRAPHY

1. A von Hippel (Edit.), Dielectric Materials and Applications, J. Wiley and Sons, Inc., New York, 1954, Chap. 2.
2. A. Oliner and H. Altschuler, "Methods of Measuring Dielectric Constants Based Upon a Microwave Network Viewpoint," J. Appl. Phys., vol. 26, pp. 214-219; February, 1955.
3. G. A. Deschamps, "Determination of Reflection Coefficients and Insertion Loss of a Waveguide Junction," J. Appl. Phys., vol. 24, pp. 1046-1050; August, 1953.
4. H. F. Mathis, "Some Properties of Image Circles," Trans. IRE, vol. MTT-4, no. 1, pp. 48-50; January, 1956.
5. E. F. Bolinder, "Impedance and Power Transformations by the Isometric Circle Method and Non-Euclidean Hyperbolic Geometry," Tech. Report 312, Research Laboratory of Electronics, M.I.T., June 14, 1957.
6. Mathis, op. cit.
7. G. A. Deschamps, op. cit.
8. J. E. Storer, L. S. Sheingold, and S. Stein, "A Simple Graphical Analysis of a Two-Port Waveguide Junction," Proc. IRE, vol. 41, pp. 1004-1013; August, 1953.
9. F. L. Wentworth and D. R. Barthel, "A Simplified Calibration of Two-Port Transmission Line Devices," IRE Trans., vol. MTT-4, no. 3, pp. 173-175; July, 1956.
10. G. A. Deschamps, "A Variant in the Measurement of Two-Port Junctions," IRE Trans., vol. MTT-5, no. 2, pp. 159-161; April, 1957.
11. E. F. Bolinder, "Impedance and Polarization-Ratio Transformations by a Graphical Method Using the Isometric Circles," Trans. IRE, vol. MTT-4, no. 3, pp. 176-180; July, 1956.
12. K. Tomiyasu, "Intrinsic Insertion Loss of a Mismatched Network," Trans. IRE, vol. MTT-3, no. 1, pp. 40-44; January, 1955.
13. Montgomery, Dicke, and Purcell, Principles of Microwave Circuits, Rad. Lab. Series, vol. 8, McGraw-Hill, New York, 1948, p. 150.

DISTRIBUTION LIST

2 Cys	Commanding Officer U.S. Army Signal Research and Development Laboratory Fort Monmouth, New Jersey ATTN: Senior Scientist Counter- measures Division	2 Cys	Commander, Wright Air Development Center Wright-Patterson Air Force Base, Ohio ATTN: WCOSI-3
1 Cy	Commanding General U.S. Army Electronic Proving Ground Fort Huachuca, Arizona ATTN: Director, Electronic Warfare Department	1 Cy	Commander, Wright Air Development Center Wright-Patterson Air Force Base, Ohio ATTN: WCLGL-7
1 Cy	Chief, Research and Development Divi- sion, Office of the Chief Signal Officer Department of the Army Washington 25, D.C. ATTN: SIGEB	1 Cy	Commander, Air Force Cambridge Research Center L.G. Hanscom Field Bedford, Massachusetts ATTN: CROTLR-2
1 Cy	Chief, Plans and Operations Division Office of the Chief Signal Officer Washington 25, D.C. ATTN: SIGEW	1 Cy	Commander, Rome Air Development Center Griffiss Air Force Base, New York ATTN: RCSSLD
1 Cy	Commanding Officer Signal Corps Electronics Research Unit 9560th USASRU, P.O. Box 205 Mountain View, California	1 Cy	Commander, Air Proving Ground Center ATTN: Adj/Technical Report Branch Eglin Air Force Base, Florida
1 Cy	U.S. Atomic Energy Commission 1901 Constitution Avenue, N.W. Washington 25, D.C. ATTN: Chief Librarian	1 Cy	Commander, Special Weapons Center Kirtland Air Force Base Albuquerque, New Mexico
1 Cy	Director, Central Intelligence Agency 2430 E Street, N.W. Washington 25, D.C. ATTN: OCD	1 Cy	Chief, Bureau of Ordnance Code ReO-1, Department of the Navy Washington 25, D.C.
1 Cy	Signal Corps Liaison Officer Lincoln Laboratory Box 73 Lexington 73, Massachusetts ATTN: Col. Clinton W. Janes	1 Cy	Chief of Naval Operations, EW Systems Branch, OP-347, Department of the Navy Washington 25, D.C.
10 Cys	Commander, Armed Services Technical Information Agency Arlington Hall Station Arlington 12, Virginia	1 Cy	Chief, Bureau of Ships, Code 840 Department of the Navy Washington 25, D.C.
1 Cy	Commander, Air Research & Development Command Andrews Air Force Base Washington 25, D.C. ATTN: RDTC	1 Cy	Chief, Bureau of Ships, Code 843 Department of the Navy Washington 25, D.C.
1 Cy	Directorate of Research & Development USAF Washington 25, D.C. ATTN: Chief, Electronic Division	1 Cy	Chief, Bureau of Aeronautics Code EL-8, Department of the Navy Washington 25, D.C.
		1 Cy	Commander, Naval Ordnance Test Station Inyokern, China Lake, California ATTN: Test Director-Code 30
		1 Cy	Commander, Naval Air Missile Test Center Point Mugu, California ATTN: Code 366

DISTRIBUTION LIST (Cont'd)

1 Cy	Commanding Officer U.S. Naval Ordnance Laboratory Silver Spring 19, Maryland	1 Cy	Stanford Electronics Laboratories Stanford University Stanford, California ATTN: Applied Electronics Laboratory Document Library
2 Cys	Chief, U.S. Army Security Agency Arlington Hall Station Arlington 12, Virginia ATTN: GAS-24L	1 Cy	HRB-Singer, Inc. Science Park State College, Penna. ATTN: R. A. Evans, Manager, Technical Information Center
1 Cy	President, U.S. Army Defense Board Headquarters Fort Bliss, Texas	1 Cy	ITT Laboratories 500 Washington Avenue Nutley 10, New Jersey ATTN: Mr. L. A. DeRosa, Div. R-15 Lab.
1 Cy	President, U.S. Army Airborne and Electronics Board Fort Bragg, North Carolina	1 Cy	The Rand Corporation 1700 Main Street Santa Monica, California ATTN: Dr. J. L. Hult
1 Cy	U.S. Army Antiaircraft Artillery and Guided Missile School Fort Bliss, Texas ATTN: E&E Dept.	1 Cy	Stanford Electronics Laboratories Stanford University Stanford, California ATTN: Dr. R. C. Cumming
1 Cy	Commander, USAF Security Service San Antonio, Texas ATTN: CLR	1 Cy	Willow Run Laboratories The University of Michigan P. O. Box 2008 Ann Arbor, Michigan ATTN: Dr. Boyd
1 Cy	Chief of Naval Research Department of the Navy Washington 25, D.C. ATTN: Code 931	1 Cy	Stanford Research Institute Menlo Park, California ATTN: Dr. Cohn
1 Cy	Commanding Officer U.S. Army Security Agency Operations Center Fort Huachuca, Arizona	2 Cys	Commanding Officer, U.S. Army Signal Missile Support Agency White Sands Missile Range, New Mexico ATTN: SIGWS-EW and SIGWS-FC
1 Cy	President, U.S. Army Security Agency Board Arlington Hall Station Arlington 12, Virginia	1 Cy	Commanding Officer, U.S. Naval Air Development Center Johnsville, Pennsylvania ATTN: Naval Air Development Center Library
1 Cy	Operations Research Office Johns Hopkins University 6935 Arlington Road Bethesda 14, Maryland ATTN: U.S. Army Liaison Officer	1 Cy	Commanding Officer, U.S. Army Signal Research & Development Laboratory Fort Monmouth, New Jersey ATTN: U.S. Marine Corps Liaison Office, Code AO-4C
1 Cy	The Johns Hopkins University Radiation Laboratory 1315 St. Paul Street Baltimore 2, Maryland ATTN: Librarian		

DISTRIBUTION LIST (Cont'd)

1 Cy	Commanding Officer, U.S. Army Signal Research & Development Laboratory Fort Monmouth, New Jersey ATTN: ARDC Liaison Office	1 Cy	Director, National Security Agency Ft. George G. Meade, Maryland ATTN: TEC
1 Cy	President, U.S. Army Signal Board Fort Monmouth, New Jersey	1 Cy	Dr. H. W. Farris, Director, Electronic Defense Group, University of Michigan Research Institute Ann Arbor, Michigan
11 Cys	Commanding Officer, U.S. Army Signal Research & Development Laboratory Fort Monmouth, New Jersey ATTN: 1 Cy - Director of Research 1 Cy - Technical Documents Center - ADT/E 1 Cy - Chief, Ctms Systems Branch, Countermeasures Division 1 Cy - Chief, Detection & Location Branch, Countermeasures Div. 1 Cy - Chief, Jamming & Deception Branch, Countermeasures Div. 1 Cy - File Unit No. 4, Mail & Records, Countermeasures Div. 1 Cy - Chief, Vulnerability Br, Electromagnetic Environment Div. 1 Cy - Reports Distribution Unit, Countermeasures Div. File 3 Cys- Chief, Security Division (for retransmittal to BJSM)	20 Cys	Electronic Defense Group Project File University of Michigan Research Institute Ann Arbor, Michigan
		1 Cy	Project File University of Michigan Research Institute Ann Arbor, Michigan
		1 Cy	Director, Air University Library Maxwell Air Force Base, Alabama ATTN: CR-4987
		1 Cy	Commanding Officer-Director U.S. Naval Electronic Laboratory San Diego 52, California
		1 Cy	Office of the Chief of Ordnance Department of the Army Washington 25, D.C. ATTN: ORDTU
		1 Cy	Chief, West Coast Office U.S. Army Signal Research and Development Laboratory Bldg. 6 75 S. Grand Avenue Pasadena 2, California
1 Cy	Director, Naval Research Laboratory Countermeasures Branch, Code 5430 Washington 25, D.C.		
1 Cy	Director, Naval Research Laboratory Washington 25, D.C. ATTN: Code 2021		

Above distribution is effected by Countermeasures Division, Surveillance Dept., USASRD, Evans Area, Belmar, New Jersey. For further information contact Mr. I. O. Myers, Senior Scientist, telephone PRospect 5-3000, Ext. 61252.

UNIVERSITY OF MICHIGAN



3 9015 03525 1654